Environmental Science & Technology Letters

Letter

Cite This: Environ. Sci. Technol. Lett. 2019, 6, 745−751

pubs.acs.org/journal/estlcu

Impact of Cu(II) and Zn(II) on the Reductive Dissolution of Pb(IV) Oxide

Weiyi Pan,[†] Lia Schattner,[†] Justin Guilak,[‡] and Daniel Giammar*[,†]

[†]Department of Energy, Environmental & Chemical Engineering, Washington University in St. Louis, St. Louis, Missouri 63130, United States

[‡]Department of Chemical & Biomolecular Engineering, Rice University, Houston, Texas 77005, United States

Supporting Information

ABSTRACT: Dissolved lead (Pb) concentrations in drinking water are mainly controlled by Pb-containing minerals in corrosion scales on lead service lines. Lead(IV) oxide (PbO_2) solids can control lead concentrations at very low values, but they are stable only in the presence of a free chlorine residual. When free chlorine is depleted, PbO_2 undergoes reductive dissolution. Zinc (Zn) and copper (Cu) may accumulate on lead-containing corrosion scales through adsorption or precipitation processes in ways that affect the rate and extent of PbO_2 dissolution. The effects of Cu(II) and Zn(II) on the reductive dissolution of PbO_2 were explored in batch experiments with PbO_2 solids and aqueous Cu(II) and Zn(II). By investigating dissolved Pb(II) concentrations with different Cu(II) and Zn(II) loadings (0−4 μM) and under different pH conditions (5.5−9.5), we found a robust inhibitory effect of Cu(II) and Zn(II) on the reductive dissolution of PbO_2. Zn(II) exhibited inhibition that was stronger than that of Cu(II). Characterization of the PbO_2 after reactions was consistent with adsorption of Cu(II) and Zn(II), leading to inhibition of PbO_2 dissolution. Under all conditions studied, α-PbO_2 dissolved faster than β-PbO_2.

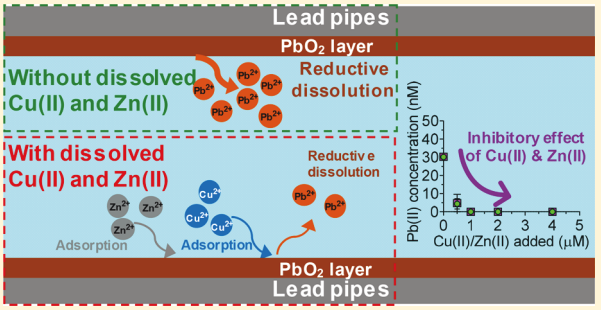

INTRODUCTION

Consumption of lead-contaminated drinking water is one of the major pathways for human exposure to lead (Pb).[1,2] Pb in drinking water is contributed by Pb-containing pipes, fittings, fixtures, and solder.[3] Millions of partial or full lead service lines (LSLs) are still present in the United States.[4] Concentrations of dissolved Pb in drinking water are mainly controlled by the solubility of Pb corrosion products that form on LSLs.[5−10] Relevant Pb corrosion products include Pb(II) carbonate solids {cerussite ($PbCO_3$) and hydrocerussite [$Pb_3(CO_3)_2(OH)_2$]}, Pb(II) oxide [litharge (PbO)], and Pb(IV) oxides [scrutinyite (α-PbO_2) and plattnerite (β-PbO_2)], as well as lead phosphate solids if phosphate is added for corrosion control.[7,8,11−14] The solubility of Pb(IV) oxide is lower than that of Pb(II) corrosion products and has been observed on LSLs that deliver drinking with free chlorine as the disinfectant.[15] The release of Pb from LSLs with scales containing Pb(IV) oxide was consistently lower than that from pipes coated with Pb(II) corrosion products.[16,17] However, PbO_2 is stable only in the high-oxidation−reduction potential (ORP) environment provided by free chlorine or in weathered hydrothermal base metal deposits.[18,19] Nearly any amount of measurable free chlorine can make PbO_2 formation energetically favorable at neutral pH, but this reaction can be kinetically limited.[6] If free chlorine is depleted, then PbO_2 may undergo reductive dissolution, which increases dissolved Pb(II) concentrations as has been observed in the field.[16] Greater and more sustained increases in lead release can occur if the residual disinfectant is switched from free chlorine to monochloramine, which provides a lower ORP. Such a switch in late 2000 in Washington, DC, induced the reductive dissolution of PbO_2 and resulted in a dramatic increase in the concentrations of Pb in water.[1,3]

The reductive dissolution of PbO_2 is promoted by reductants such as natural organic matter (NOM), I^-, Mn^{2+}, and Fe^{2+}.[20−23] The reduction of PbO_2 by water is even thermodynamically favorable.[18] PbO_2 reductive dissolution involves a coupled reduction−detachment process, and the dissolution rate has been shown to be proportional to the concentrations of Pb(IV) surface species as shown in eqs 1−3.[24] These reactions can predict the surface speciation of PbO_2 as a function of pH, and $\equiv Pb(IV)O^-$ is reduced the fastest. Adsorption or precipitation of Ca(II) and Pb(II) on the PbO_2 surface can decrease the concentrations of Pb(IV) surface species and inhibit the reductive dissolution of PbO_2.[22,24] Shi and Stone observed that 0.1 mM Ca^{2+} decreased the rate of reductive dissolution of PbO_2 by hydroquinone via precipitation of Ca(II)-containing solids on the PbO_2 surface.[22] Adsorption of Pb(II) also inhibited PbO_2 dissolution by

Received: September 30, 2019
Revised: November 11, 2019
Accepted: November 12, 2019
Published: November 14, 2019

DOI: 10.1021/acs.estlett.9b00612
Environ. Sci. Technol. Lett. 2019, 6, 745−751

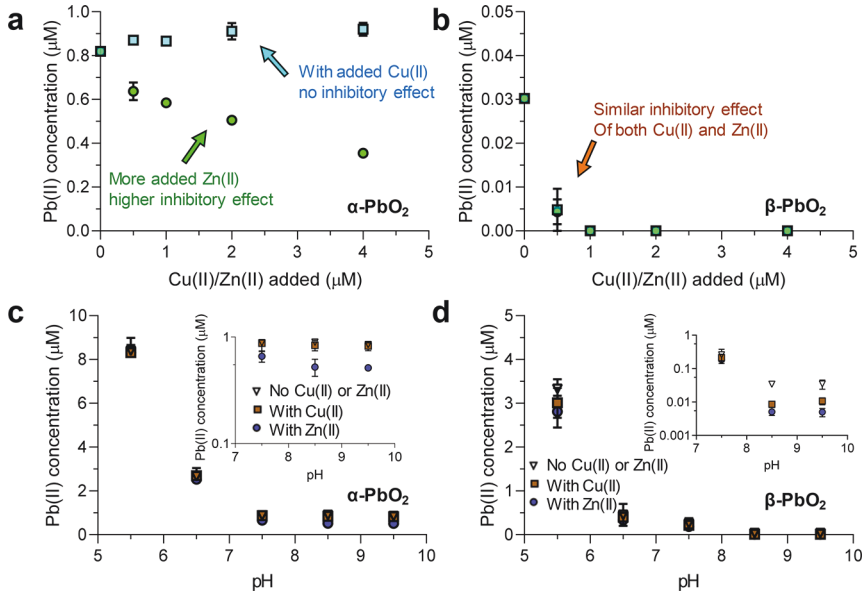

Figure 1. Effect of different Cu(II) and Zn(II) concentrations (0−4 μM) on (a) α-PbO_2 and (b) β-PbO_2 dissolution at pH 8.5 ± 0.2 and effect of pH (5.5−9.5) on (c) α-PbO_2 and (d) β-PbO_2 dissolution with 2 μM Cu(II) and Zn(II). The experiments were conducted with an initial DIC of 4.2 mM, 0.01 M ionic strength $NaNO_3$, and 0.05 g/L PbO_2 and buffered at the target pH with 2 mM MOPS. The average values from duplicate experiments after 12 h are shown, and the error bars represent the standard deviation from the duplicate experiments. To illustrate the differences in the extents of dissolution among different conditions in panels c and d, insets of the data are presented that plot the data using a logarithmic scale for the lead concentration. The triangles, squares, and circles in panels c and d mean no Cu(II) or Zn(II), with 2 μM Cu(II), and with 2 μM Zn(II), respectively.

forming a Pb(II) surface complex (eq 3) that altered the distribution of surface Pb(IV) species.[24] Other cations may have even greater inhibitory effects on PbO_2 reductive dissolution than do Pb(II) species and Ca^{2+}, but they have not been comprehensively investigated.

$$\equiv Pb(IV)OH_2^+ \leftrightarrow \equiv Pb(IV)OH + H^+ \quad (1)$$

$$\equiv Pb(IV)OH \leftrightarrow \equiv Pb(IV)O^- + H^+ \quad (2)$$

$$\equiv Pb(IV)O^- + Pb^{2+} \leftrightarrow \equiv Pb(IV)OPb^+ \quad (3)$$

Zinc (Zn) and copper (Cu) are common elements present in brass pipes and fittings used for drinking water supply.[25−27] Previous studies found that Zn [such as smithsonite ($ZnCO_3$)] and Cu {such as malachite [$Cu_2CO_3(OH)_2$], brochantite [$Cu_4SO_4(OH)_6$], and antlerite [$Cu_3SO_4(OH)_4$]} can accumulate in corrosion scales on LSLs.[12] Zn(II) and Cu(II) released by these scales may be adsorbed onto metal oxides, including PbO_2, present on pipe surfaces.[28] The presence of Cu(II) and Zn(II) may alter the surface speciation of PbO_2 in a way that decreases the rate of release of Pb(II) to water.

The objectives of this study were to determine the effects of Zn(II) and Cu(II) on PbO_2 reductive dissolution and delineate the adsorption behavior of Zn(II) and Cu(II) on PbO_2. Experiments were performed over a range of environmentally relevant conditions with both polymorphs of PbO_2 (α-PbO_2 and β-PbO_2) that are found as corrosion products.[10,16,29] Solids were characterized before and after reactions to explore the inhibitory mechanism of Cu(II) and Zn(II).

MATERIALS AND METHODS

Materials. Plattnerite (β-PbO_2) was purchased from Fisher Scientific. Scrutinyite (α-PbO_2) was synthesized using a published method.[6] The purities of synthesized α-PbO_2 and purchased β-PbO_2 were confirmed by X-ray diffraction (XRD) (Figure S1) and X-ray photoelectron spectroscopy (XPS) (Figure S2). The specific surface areas of α-PbO_2 and β-PbO_2 were 5.5 and 4.2 m^2/g, respectively, as measured by BET-N_2 adsorption. Other chemicals used in this study are listed in the Supporting Information.

PbO_2 Reductive Dissolution with Different Cu(II) and Zn(II) Loadings. To investigate the effect of different Cu(II) and Zn(II) loadings [0−4 μM, 0−256 μg/L for Cu(II) and 0−260 μg/L for Zn(II)] on the reductive dissolution of PbO_2, we conducted a series of batch experiments with 0.05 g/L PbO_2 suspensions. The concentration of PbO_2 was selected as 0.05 g/L to provide sufficient PbO_2 for measurable results and to prevent the possibility of complete consumption of PbO_2. The ionic strength (IS) was controlled at 0.01 M by $NaNO_3$. The addition of $NaHCO_3$ maintained an environmentally relevant dissolved inorganic carbon (DIC) concentration of 50 mg/L (4.2 mM) as C. The pH was buffered at 8.5 ± 0.2 with 2 mM 3-(*N*-morpholino)propanesulfonic (MOPS) (pK_a = 7.2). A pH of 8.5 was selected because it is environmentally relevant and the inhibitory effect of Cu(II) and Zn(II) is significant under this condition. MOPS was employed as a pH buffer because it has a high buffer capacity at our target pH values and was previously found to have a weak effect on PbO_2 dissolution.[23] Although $NaNO_3$ and MOPS are not constituents in drinking water, they helped maintain a relevant pH and ionic strength. Aqueous samples were taken at 0, 1, 2, 6, and 12 h for total dissolved Pb, Cu, and Zn analysis to track the extents of PbO_2 dissolution and Cu and Zn uptake. All of the reagents except PbO_2 were added to the solution first, and the timer was started after the addition of the PbO_2 stock solution. The Pb concentrations at 12 h were used to assess differences in the extent of dissolution among different conditions. The O_2 levels during the experiments were not tracked because our system was not strictly a closed system. At the beginning and end of

DOI: 10.1021/acs.estlett.9b00612
Environ. Sci. Technol. Lett. 2019, 6, 745−751

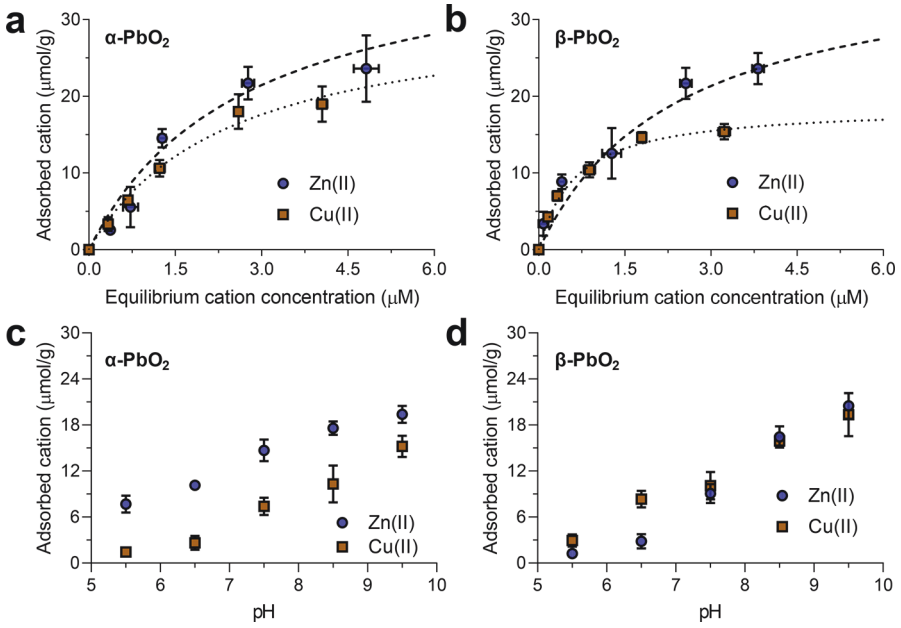

Figure 2. Adsorption isotherms of Cu(II) and Zn(II) on α-PbO_2 and β-PbO_2 (a and b, respectively) at pH 8.5 ± 0.2 and effect of pH on adsorption of 2 μM Cu(II) and Zn(II) on α-PbO_2 and β-PbO_2 (c and d, respectively). Experimental results are shown as solid points, and the outputs of a Langmuir adsorption isotherm are shown as dashed lines. The experiments were conducted with an initial DIC of 4.2 mM, 0.01 M ionic strength $NaNO_3$, and 0.05 g/L PbO_2 and buffered at the target pH with 2 mM MOPS. The average values from duplicate experiments after 12 h are shown, and the error bars represent the standard deviation from the duplicate experiments.

the experiment, samples of suspension were collected, centrifuged, and freeze-dried to yield solids for XPS and XRD characterization.

Effect of pH on PbO_2 Reductive Dissolution with 2 μM Cu(II) and Zn(II). Reductive dissolution of PbO_2 was examined for pH values between 5.5 and 9.5 (buffered with 2 mM MOPS) with a solid loading of 0.05 g/L PbO_2. The ionic strength was controlled at 0.01 M by $NaNO_3$ and an initial DIC concentration of 50 mg/L (4.2 mM) as C. The solutions were sealed in 100 mL polypropylene bottles to minimize CO_2 exchange with the atmosphere. Although MOPS provided little buffering at pH 5.5 or 9.5, it was used in all experiments to maintain a constant concentration. Initial Cu(II) and Zn(II) concentrations in the solution were controlled at 2 μM [128 μg/L for Cu(II) and 130 μg/L for Zn(II)]. Aqueous samples were taken at 0, 1, 2, 6, and 12 h for Pb(II), Cu(II), and Zn(II) analysis.

All experiments were performed in duplicate reactors that were continuously stirred with polypropylene-coated stir bars at a speed of 500 rpm on a multiposition stirrer (VARIOMAG, Thermo) at room temperature (21 ± 1 °C). Sample pretreatment methods for ICP-MS analysis are described in the Supporting Information. Cu(II) and Zn(II) species under different pH conditions were calculated by Visual MINTEQ 3.1.[30] Additional details of instrumental analysis are provided in the Supporting Information.

RESULTS AND DISCUSSION

Reductive Dissolution of Two PbO_2 Polymorphs with Cu(II) and Zn(II). Cu(II) and Zn(II) inhibited the reductive dissolution of both α-PbO_2 and β-PbO_2 at pH 8.5 (Figure 1a,b and Figure S3). For α-PbO_2, less Pb(II) was detected at 12 h in the presence of Zn(II), and the inhibitory effect increased with an increase in Zn(II) concentration. With 4 μM Zn(II) (260 μg/L), the level of reductive dissolution of α-PbO_2 was 67% less than without Zn(II). Reductive dissolution of β-PbO_2 was even more significantly inhibited, and no dissolved Pb was detected when >1 μM Cu(II) (64 μg/L) or Zn(II) (65 μg/L) was added to the solution. Significant inhibitory effects of Cu(II) and Zn(II) on PbO_2 reductive dissolution were observed at pH 7.5−9.5. However, when the pH was <7.5 (pH 5.5 and 6.5), no significant inhibitory effects were observed in the presence of 2 μM Cu(II) (128 μg/L) or Zn(II) (130 μg/L) (Figure 1c,d and Figure S4). PbO_2 reductive dissolution may be so much faster at pH 6.5 that any inhibition cannot be detected. Cu(II) and Zn(II) also may not adsorb sufficiently to PbO_2 to have an inhibitory effect. These two hypotheses for the lack of an inhibitory effect of Cu(II) and Zn(II) at pH 5.5 and 6.5 are explored further below. Similar effects of pH on reductive dissolution have been observed with other metal oxides such as goethite, hydrous Fe(III) oxides, and Mn oxides.[31−34]

The inhibitory effect of Cu(II) was due to the adsorption of Cu(II) on the β-PbO_2 surface. When the Cu(II) concentration was ≤2 μM, the system was undersaturated with respect to $Cu_2(OH)_2CO_{3(s)}$ (as shown in Figure S5), and the inhibitory effect can be attributed to the adsorption of Cu(II). For experiments with 4 μM Cu(II), the formation of $Cu_2(OH)_2CO_{3(s)}$ is thermodynamically favorable, but no precipitation was observed in the PbO_2-free control experiments. Consequently, it is likely that the inhibitory effect was still due to the adsorption of Cu(II) on β-PbO_2. XRD was not conducted to probe for the formation of $Cu_2CO_3(OH)_{2(s)}$ because even if all of the Cu(II) had precipitated, the amount of $Cu_2CO_3(OH)_{2(s)}$ would still be below the detection limit (~1% by mass). The experiments with Zn(II) had solutions that were undersaturated with respect to $ZnCO_{3(s)}$ and $Zn(OH)_{2(s)}$ under all experimental conditions. Scanning electron microscopy (SEM) images (Figure S6) were consistent with the conclusion that no secondary precipitates

DOI: 10.1021/acs.estlett.9b00612
Environ. Sci. Technol. Lett. 2019, 6, 745−751

formed during the experiments. As a result, the inhibitory effect was attributed to the adsorption of Zn(II) and not to precipitation.

The rates and extents at 12 h of reductive dissolution of α-PbO_2 were much higher than those of β-PbO_2 (as shown in Figures S3 and S4 and Figure 1). The differences between α-PbO_2 and β-PbO_2 reductive dissolution kinetics may have two causes. First, the different reductive dissolution rates of these solids could be associated with different thermodynamic stabilities. Previous studies have shown that β-PbO_2 is more thermodynamically stable than α-PbO_2,[6,14,15,18,35] which is consistent with our observed reductive dissolution rates of α-PbO_2 and β-PbO_2. Second, differences in Pb oxidation states in the two PbO_2 polymorphs may affect the rates of reductive dissolution. The Pb oxidation state in PbO_2 is not exactly +4 because of Pb(II) defects in the PbO_2 crystalline structures. According to Guo et al., α-PbO_2 has a higher average Pb oxidation state (+3.86) than β-PbO_2 (+3.81), which indicates a higher oxidation activity for α-PbO_2.[35]

Adsorption of Zn(II) and Cu(II) on Two PbO_2 Polymorphs. The equilibrium relationships between dissolved and adsorbed Zn(II) and Cu(II) concentrations were best captured by the Langmuir isotherm for both α-PbO_2 and β-PbO_2 (Figure 2a,b). The adsorption of Zn(II) and Cu(II) on α-PbO_2 and β-PbO_2 reached equilibrium around 2 h (Figure S7). The adsorption of Zn(II) is more favorable than that of Cu(II) on both α-PbO_2 and β-PbO_2. The α-PbO_2 showed maximum adsorption capacities of 38.6 and 40.7 μmol/g (7.0 and 7.4 μmol/m^2) for Cu(II) and Zn(II), respectively, while β-PbO_2 exhibited maximum adsorption capacities of 18.7 and 31.9 μmol/g (4.45 and 7.6 μmol/m^2) for Cu(II) and Zn(II), respectively. The maximum adsorption capacities were on the same order of magnitude, and the ones for Zn(II) are nearly identical for α-PbO_2 and β-PbO_2. The Zn(II) and Cu(II) adsorption capacities observed here are within the range of what has previously been observed (1−13 μmol/m^2) on other metal oxides such as hematite, goethite, and hydrous manganese dioxide.[36−39] Because the experiments were performed at pH values of 5.5−9.5 that were all above the reported range of pHpzc values for α-PbO_2 and β-PbO_2 (4.8−5.2),[23,24] the surfaces of the solids were negatively charged. As shown in Figure S8, Cu^{2+}, $CuCO_{3(aq)}$, and $Cu(CO_3)_2^{2-}$ were the main dissolved Cu(II) species at pH 5.5−6.5, 7.5−8.5, and 9.5, respectively. For Zn(II), Zn^{2+}, $ZnCO_{3(aq)}$, and $Zn(OH)_{2(aq)}$ were the main species at pH 5.5−7.5, 8.5, and 9.5, respectively. An initial DIC concentration of 4.2 mM was added to all solutions. Because of the opening of reactors during sampling and pH measurements, our systems were not strictly closed to the atmosphere so the DIC concentration could have deviated from its initial value. While the proportions of species change depending on whether the system is open or closed with respect to atmospheric CO_2, for a given pH the dominant Cu(II) species are the same regardless of whether the system is open or closed, and with the exception of pH 9.5, the dominant Zn(II) species are also the same for open and closed systems for a given pH (Figures S8 and S9). Although this DIC concentration probably cannot be maintained at pH 5.5 and 6.5, it does not affect our overall interpretation because DIC has almost no effect on Cu(II) and Zn(II) speciation at pH ≤6.5.

The adsorption extents of Cu(II) and Zn(II) on α-PbO_2 and β-PbO_2 increased with an increase in pH from 5.5 to 9.5, as shown in panels c and d of Figure 2 and Figure S10. As shown in eqs 4 and 5, a higher pH favors a greater level of formation of Cu(II) and Zn(II) surface complexes. On the basis of previous studies of adsorption to other metal oxides, Cu(II) and Zn(II) adsorption is expected to increase with an increase in pH.[37−41]

$$\equiv Pb(IV)O^- + Cu^{2+} \leftrightarrow \equiv Pb(IV)OCu^+ \quad (4)$$

$$\equiv Pb(IV)O^- + Zn^{2+} \leftrightarrow \equiv Pb(IV)OZn^+ \quad (5)$$

XPS was used to determine the oxidation state of lead at the PbO_2 surface (Figure 3) and to identify any changes in the abundances of elements on the exposed surfaces (top 1−10 nm) of the solids before and after the experiments (Figure S11). Before the experiment, the Pb 4f spectrum of both α-PbO_2 and β-PbO_2 consisted of a spin−orbit doublet each displaying an asymmetric peak shape with peak binding energies for Pb $4f_{7/2}$ and Pb $4f_{5/2}$ (Figure 3) at 137.5 and 142.5 eV, respectively. These characteristics were in good agreement with previous reports.[20,42] In the presence of Cu(II) and Zn(II), the peak shapes of Pb $4f_{7/2}$ did not change after 12 h, which suggests that Pb(II) generated by reduction of PbO_2 was released to the solution and that no Pb(II) precipitation occurred within 12 h. The uptake of Zn(II) and Cu(II) onto α-PbO_2 and β-PbO_2 surfaces could also be detected by XPS (Figure S11).

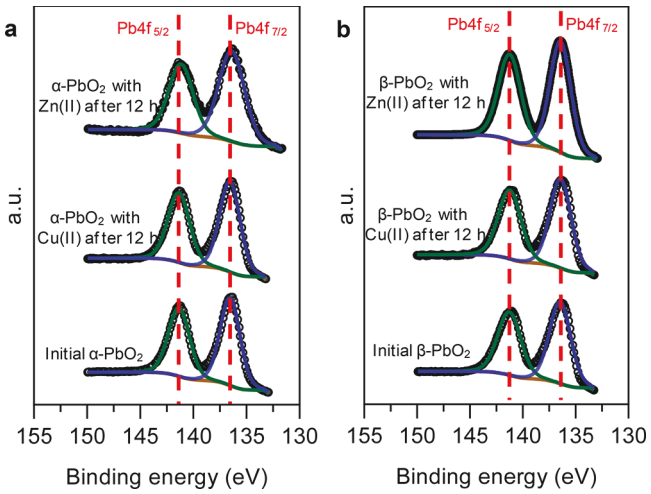

Figure 3. XPS spectra of the Pb 4f region of (a) α-PbO_2 and (b) β-PbO_2 before and after adsorption experiments. The experiments were conducted with 4.2 mM C/L as DIC, 0.05 g/L PbO_2, and 0.01 M ionic strength $NaNO_3$ and buffered at pH 8.5 ± 0.2 with 2 mM MOPS. The initial Cu(II) and Zn(II) concentrations were 4 μM. All spectra are energy-corrected by setting the C 1s peak equal to 284.8 eV. a.u. stands for arbitrary unit.

Mechanism of the Cu(II) and Zn(II) Inhibitory Effect on PbO_2 Reductive Dissolution. The reductive dissolution of PbO_2 has been described as occurring in three steps: (1) reductant adsorption to the PbO_2 surface, (2) electron transfer between the reductants and the PbO_2 that generates Pb(II) on the PbO_2 surface, and (3) detachment of the Pb(II) to solution.[20,43] When the reductant is water, these processes can be simplified by a coupled process of electron transfer and Pb(II) detachment because water molecules will always be at the PbO_2 surface.[24] In this process, Pb(III) may form as an unstable intermediate species.[44,45] The experimental results suggested that the inhibitory effect of Cu(II) and Zn(II) can

DOI: 10.1021/acs.estlett.9b00612
Environ. Sci. Technol. Lett. 2019, 6, 745−751

be attributed to their adsorption onto the PbO_2 surface. Although our dissolution and adsorption results did not provide molecular-scale evidence of the inhibitory mechanism, there are two plausible hypotheses. First, the reactive surface sites that control PbO_2 reductive dissolution are the same ones to which Zn(II) and Cu(II) adsorption occurred. Zn(II) and Cu(II) could strongly adsorb to the PbO_2 surface (eqs 4 and 5) to block access to surface sites where Pb(IV) reduction would occur. Similar effects have been observed with layered Mn(IV) oxides with adsorption of metal cations increasing the stability of layered Mn(IV) oxides.[46] Second, PbO_2 may structurally incorporate Cu(II) and Zn(II) to form more thermodynamically stable solids. Redox-driven recrystallization may happen between PbO_2 and Pb(II) in a process similar to that which occurs for Fe(II) with Fe(III) oxides and Mn(II) with manganite.[47−51] Cations that include Ni(II), Cu(II), Ca(II), and Zn(II) can be incorporated into the structures of the manganite and Fe(III) oxides during the recrystallization processes.[52−54] To test these hypotheses, X-ray absorption fine structure (XAFS) spectroscopy could be conducted in future research with PbO_2 harvested from adsorption experiments to distinguish Cu(II) or Zn(II) adsorption and incorporation.

Environmental Implications. The reductive dissolution of PbO_2 on LSLs when free chlorine is depleted can be a major source of Pb(II) in drinking water. Our experiments indicate that Cu(II) and Zn(II) released by Cu- and Zn-containing materials may adsorb to PbO_2 and increase its resistance to reductive dissolution or alter the surface chemistry,[55,56] thereby helping maintain low Pb concentrations in water. The equilibrium time for these reactions also suggests that the stagnation time prior to sampling from real LSLs should depend on the time required for free chlorine depletion to occur. This study may help explain the observation of β-PbO_2 as the dominant Pb(IV) oxide on LSLs in field studies,[8,10,16,57] while laboratory-scale experiments observed the formation of both α-PbO_2 and β-PbO_2.[6,15] The reductive dissolution rate and extent of α-PbO_2 are much higher than those of β-PbO_2. In the presence of Cu(II) and Zn(II), the stability of β-PbO_2 also increases more than that of α-PbO_2.

■ ASSOCIATED CONTENT

Supporting Information

The Supporting Information is available free of charge on the ACS Publications website at DOI: 10.1021/acs.estlett.9b00612.

Chemicals used in this study, sample pretreatment methods for ICP-MS, additional details of instrumental analysis, 11 figures showing the XRD and XPS characterization of the solids, dissolution kinetic results of PbO_2 under experimental conditions, predicted solubility and aqueous speciation of Zn(II) and Cu(II), SEM images of solids, and adsorption of Cu(II) and Zn(II) on PbO_2 under experimental conditions (PDF)

■ AUTHOR INFORMATION

Corresponding Author

*Campus Box 1180, One Brookings Drive, St. Louis, MO 63130. Phone: 314-935-6849. Fax: 314-935-7211. E-mail: giammar@wustl.edu.

ORCID

Weiyi Pan: 0000-0001-6587-1040

Daniel Giammar: 0000-0002-4634-5640

Notes

The authors declare no competing financial interest.

■ ACKNOWLEDGMENTS

This research was supported by the U.S. National Science Foundation (CBET 1603717 and CHE 1709484). W.P. acknowledges the fellowship support through the McDonnell International Scholars Academy. This work was performed in part using the Nanoscale Research Facility at Washington University in St. Louis, a member of the National Nanotechnology Infrastructure Network (NNIN), which was supported by the National Science Foundation under Grant ECCS-0335765. The authors thank Anushka Mishrra, Anshuman Satpathy, and Yeunook Bae for assistance with experimental activities and Dr. Jeff Catalano and Neha Sharma for helpful discussions.

■ REFERENCES

(1) Edwards, M.; Triantafyllidou, S.; Best, D. Elevated Blood Lead in Young Children Due to Lead-Contaminated Drinking Water: Washington, DC, 2001− 2004. *Environ. Sci. Technol.* **2009**, *43*, 1618−1623.

(2) Triantafyllidou, S.; Edwards, M. Lead (Pb) in Tap Water and in Blood: Implications for Lead Exposure in the United States. *Crit. Rev. Environ. Sci. Technol.* **2012**, *42*, 1297−1352.

(3) Edwards, M.; Dudi, A. Role of Chlorine and Chloramine in Corrosion of Lead-Bearing Plumbing Materials. *J. - Am. Water Works Assoc.* **2004**, *96*, 69−81.

(4) Cornwell, D. A.; Brown, R. A.; Via, S. H. National Survey of Lead Service Line Occurrence. *J. - Am. Water Works Assoc.* **2016**, *108*, E182−E191.

(5) Schock, M. R. Understanding Corrosion Control Strategies for Lead. *J. - Am. Water Works Assoc.* **1989**, *81*, 88−100.

(6) Wang, Y.; Xie, Y.; Li, W.; Wang, Z.; Giammar, D. E. Formation of Lead (IV) Oxides from Lead (II) Compounds. *Environ. Sci. Technol.* **2010**, *44*, 8950−8956.

(7) Del Toral, M. A.; Porter, A.; Schock, M. R. Detection and Evaluation of Elevated Lead Release from Service Lines: A Field Study. *Environ. Sci. Technol.* **2013**, *47*, 9300−9307.

(8) DeSantis, M. K.; Triantafyllidou, S.; Schock, M. R.; Lytle, D. A. Mineralogical Evidence of Galvanic Corrosion in Drinking Water Lead Pipe Joints. *Environ. Sci. Technol.* **2018**, *52*, 3365−3374.

(9) Peng, C.-Y.; Korshin, G. V.; Valentine, R. L.; Hill, A. S.; Friedman, M. J.; Reiber, S. H. Characterization of Elemental and Structural Composition of Corrosion Scales and Deposits Formed in Drinking Water Distribution Systems. *Water Res.* **2010**, *44*, 4570−4580.

(10) Kim, E. J.; Herrera, J. E. Characteristics of Lead Corrosion Scales Formed during Drinking Water Distribution and Their Potential Influence on the Release of Lead and Other Contaminants. *Environ. Sci. Technol.* **2010**, *44*, 6054−6061.

(11) Frenkel, A. I.; Korshin, G. V. EXAFS Studies of the Chemical State of Lead and Copper in Corrosion Products Formed on the Brass Surface in Potable Water. *J. Synchrotron Radiat.* **1999**, *6*, 653−655.

(12) Schock, M. R.; Hyland, R. N.; Welch, M. M. Occurrence of Contaminant Accumulation in Lead Pipe Scales from Domestic Drinking-Water Distribution Systems. *Environ. Sci. Technol.* **2008**, *42*, 4285−4291.

(13) Schock, M. R. Response of Lead Solubility to Dissolved Carbonate in Drinking Water. *J. - Am. Water Works Assoc.* **1980**, *72*, 695−704.

(14) Liu, H.; Korshin, G. V.; Ferguson, J. F. Investigation of the Kinetics and Mechanisms of the Oxidation of Cerussite and Hydrocerussite by Chlorine. *Environ. Sci. Technol.* **2008**, *42*, 3241−3247.

(15) Lytle, D. A.; Schock, M. R. Formation of Pb(IV) Oxides in Chlorinated Water. *J. - Am. Water Works Assoc.* **2005**, *97*, 102−114.

DOI: 10.1021/acs.estlett.9b00612
Environ. Sci. Technol. Lett. 2019, 6, 745−751

(16) Triantafyllidou, S.; Schock, M. R.; Desantis, M. K.; White, C. Low Contribution of PbO_2-Coated Lead Service Lines to Water Lead Contamination at the Tap. *Environ. Sci. Technol.* **2015**, *49*, 3746−3754.
(17) Bae, Y.; Liu, V.; Pasteris, J.; Giammar, D. Effectiveness of Orthophosphate Addition for Controlling Lead Levels in Water Conveyed through Lead Service Lines during a Switch in Disinfectant. *Abstracts of Papers of the American Chemical Society* **2019**, *257*, 260.
(18) Pan, W.; Pan, C.; Bae, Y.; Giammar, D. Role of Manganese in Accelerating the Oxidation of Pb(II) Carbonate Solids to Pb(IV) Oxide at Drinking Water Conditions. *Environ. Sci. Technol.* **2019**, *53*, 6699−6707.
(19) Anthony, J. W.; Bideaux, R. A.; Bladh, K. W.; Nichols, M. C. *Handbook of mineralogy*; Mineral Data Publications: Tucson, AZ, 1990; Vol. *1*.
(20) Lin, Y. P.; Valentine, R. L. The Release of Lead from the Reduction of Lead Oxide (PbO_2) by Natural Organic Matter. *Environ. Sci. Technol.* **2008**, *42*, 760−765.
(21) Lin, Y. P.; Washburn, M. P.; Valentine, R. L. Reduction of Lead Oxide (PbO_2) by Iodide and Formation of Iodoform in the PbO_2/I-/NOM System. *Environ. Sci. Technol.* **2008**, *42*, 2919−2924.
(22) Shi, Z.; Stone, A. T. PbO_2 (s, Plattnerite) Reductive Dissolution by Natural Organic Matter: Reductant and Inhibitory Subfractions. *Environ. Sci. Technol.* **2009**, *43*, 3604−3611.
(23) Shi, Z.; Stone, A. T. PbO_2 (s, Plattnerite) Reductive Dissolution by Aqueous Manganous and Ferrous Ions. *Environ. Sci. Technol.* **2009**, *43*, 3596−3603.
(24) Wang, Y.; Wu, J.; Wang, Z.; Terenyi, A.; Giammar, D. E. Kinetics of Lead (IV) Oxide (PbO_2) Reductive Dissolution: Role of Lead(II) Adsorption and Surface Speciation. *J. Colloid Interface Sci.* **2013**, *389*, 236−243.
(25) Hill, A. S.; Friedman, M. J.; Reiber, S. H.; Korshin, G. V.; Valentine, R. L. Behavior of Trace Inorganic Contaminants in Drinking Water Distribution Systems. *J. - Am. Water Works Assoc.* **2010**, *102*, 107−118.
(26) Sarver, E.; Zhang, Y.; Edwards, M. Review of Brass Dezincification Corrosion in Potable Water Systems. *Corros. Rev.* **2010**, *28*, 155−196.
(27) Boulay, N.; Edwards, M. Role of Temperature, Chlorine, and Organic Matter in Copper Corrosion by-Product Release in Soft Water. *Water Res.* **2001**, *35*, 683−690.
(28) Stumm, W.; Morgan, J. J. *Aquatic Chemistry: Chemical Equilibria and Rates in Natural Waters*, 3rd ed.; Wiley: New York, 1996.
(29) Schock, M. R.; Harmon, S. M.; Swertfeger, J.; Lohmann, R. Tetravalent Lead: A Hitherto Unrecognized Control of Tap Water Lead Contamination. Water Quality Technology Conference, Nashville, TN, November 11−14, 2001; pp 2270−2291.
(30) Gustafsson, J. P. *Visual MINTEQ*, version 3.1; KTH: Royal Institute of Technology: Stockholm, 2013.
(31) Stone, A. T. Reductive Dissolution of Manganese(III/IV) Oxides by Substituted Phenols. *Environ. Sci. Technol.* **1987**, *21*, 979−988.
(32) LaKind, J. S.; Stone, A. T. Reductive Dissolution of Goethite by Phenolic Reductants. *Geochim. Cosmochim. Acta* **1989**, *53*, 961−971.
(33) Suter, D.; Banwart, S.; Stumm, W. Dissolution of Hydrous Iron(III) Oxides by Reductive Mechanisms. *Langmuir* **1991**, *7*, 809−813.
(34) Stone, A. T. Microbial Metabolites and the Reductive Dissolution of Manganese Oxides: Oxalate and Pyruvate. *Geochim. Cosmochim. Acta* **1987**, *51*, 919−925.
(35) Guo, D.; Robinson, C.; Herrera, J. E. Role of Pb(II) Defects in the Mechanism of Dissolution of Plattnerite (β-PbO_2) in Water under Depleting Chlorine Conditions. *Environ. Sci. Technol.* **2014**, *48*, 12525−12532.
(36) Benjamin, M. M.; Leckie, J. O. Multiple-Site Adsorption of Cd, Cu, Zn, and Pb on Amorphous Iron Oxyhydroxide. *J. Colloid Interface Sci.* **1981**, *79*, 209−221.
(37) Grossl, P. R.; Sparks, D. L.; Ainsworth, C. C. Rapid Kinetics of Cu(II) Adsorption/Desorption on Goethite. *Environ. Sci. Technol.* **1994**, *28*, 1422−1429.
(38) Su, Q.; Pan, B.; Wan, S.; Zhang, W.; Lv, L. Use of Hydrous Manganese Dioxide as a Potential Sorbent for Selective Removal of Lead, Cadmium, and Zinc Ions from Water. *J. Colloid Interface Sci.* **2010**, *349*, 607−612.
(39) Chen, Y. H.; Li, F. A. Kinetic Study on Removal of Copper(II) Using Goethite and Hematite Nano-Photocatalysts. *J. Colloid Interface Sci.* **2010**, *347*, 277−281.
(40) Hua, M.; Zhang, S.; Pan, B.; Zhang, W.; Lv, L.; Zhang, Q. Heavy Metal Removal from Water/Wastewater by Nanosized Metal Oxides: A Review. *J. Hazard. Mater.* **2012**, *211*−*212*, 317−331.
(41) Pan, B.; Qiu, H.; Pan, B.; Nie, G.; Xiao, L.; Lv, L.; Zhang, W.; Zhang, Q.; Zheng, S. Highly Efficient Removal of Heavy Metals by Polymer-Supported Nanosized Hydrated Fe(III) Oxides: Behavior and XPS Study. *Water Res.* **2010**, *44*, 815−824.
(42) Ng, D. Q.; Strathmann, T. J.; Lin, Y. P. Role of Orthophosphate as a Corrosion Inhibitor in Chloraminated Solutions Containing Tetravalent Lead Corrosion Product PbO_2. *Environ. Sci. Technol.* **2012**, *46*, 11062−11069.
(43) Wang, Y.; Wu, J.; Giammar, D. E. Kinetics of the Reductive Dissolution of Lead(IV) Oxide by Iodide. *Environ. Sci. Technol.* **2012**, *46*, 5859−5866.
(44) Elzinga, E. J. 54Mn Radiotracers Demonstrate Continuous Dissolution and Reprecipitation of Vernadite (δ-MnO_2) during Interaction with Aqueous Mn(II). *Environ. Sci. Technol.* **2016**, *50*, 8670−8677.
(45) Elzinga, E. J.; Kustka, A. B. A Mn-54 Radiotracer Study of Mn Isotope Solid-Liquid Exchange during Reductive Transformation of Vernadite (δ-MnO_2) by Aqueous Mn(II). *Environ. Sci. Technol.* **2015**, *49*, 4310−4316.
(46) Yang, P.; Post, J. E.; Wang, Q.; Xu, W.; Geiss, R.; McCurdy, P. R.; Zhu, M. Metal Adsorption Controls Stability of Layered Manganese Oxides. *Environ. Sci. Technol.* **2019**, *53*, 7453−7462.
(47) Frierdich, A. J.; Helgeson, M.; Liu, C.; Wang, C.; Rosso, K. M.; Scherer, M. M. Iron Atom Exchange between Hematite and Aqueous Fe(II). *Environ. Sci. Technol.* **2015**, *49*, 8479−8486.
(48) Handler, R. M.; Frierdich, A. J.; Johnson, C. M.; Rosso, K. M.; Beard, B. L.; Wang, C.; Latta, D. E.; Neumann, A.; Pasakarnis, T.; Premaratne, W. A. P. J.; et al. Fe(II)-Catalyzed Recrystallization of Goethite Revisited. *Environ. Sci. Technol.* **2014**, *48*, 11302−11311.
(49) Taylor, S. D.; Liu, J.; Zhang, X.; Arey, B. W.; Kovarik, L.; Schreiber, D. K.; Perea, D. E.; Rosso, K. M. Visualizing the Iron Atom Exchange Front in the Fe(II)-Catalyzed Recrystallization of Goethite by Atom Probe Tomography. *Proc. Natl. Acad. Sci. U. S. A.* **2019**, *116*, 2866−2874.
(50) Gorski, C. A.; Handler, R. M.; Beard, B. L.; Pasakarnis, T.; Johnson, C. M.; Scherer, M. M. Fe Atom Exchange between Aqueous Fe^{2+} and Magnetite. *Environ. Sci. Technol.* **2012**, *46*, 12399−12407.
(51) Frierdich, A. J.; Spicuzza, M. J.; Scherer, M. M. Oxygen Isotope Evidence for Mn(II)-Catalyzed Recrystallization of Manganite (γ-MnOOH). *Environ. Sci. Technol.* **2016**, *50*, 6374−6380.
(52) Hinkle, M. A. G.; Dye, K. G.; Catalano, J. G. Impact of Mn(II)-Manganese Oxide Reactions on Ni and Zn Speciation. *Environ. Sci. Technol.* **2017**, *51*, 3187−3196.
(53) Lefkowitz, J. P.; Elzinga, E. J. Impacts of Aqueous Mn(II) on the Sorption of Zn(II) by Hexagonal Birnessite. *Environ. Sci. Technol.* **2015**, *49*, 4886−4893.
(54) Frierdich, A. J.; Luo, Y.; Catalano, J. G. Trace Element Cycling through Iron Oxide Minerals during Redox-Driven Dynamic Recrystallization. *Geology* **2011**, *39*, 1083−1086.
(55) Ma, X.; Armas, S. M.; Soliman, M.; Lytle, D. A.; Chumbimuni-Torres, K.; Tetard, L.; Lee, W. H. In Situ Monitoring of Pb^{2+} Leaching from the Galvanic Joint Surface in a Prepared Chlorinated Drinking Water. *Environ. Sci. Technol.* **2018**, *52*, 2126−2133.
(56) Ma, X.; Lytle, D. A.; Lee, W. H. Microelectrode Investigation on the Corrosion Initiation at Lead−Brass Galvanic Interfaces in Chlorinated Drinking Water. *Langmuir* **2019**, *35*, 12947−12954.

DOI: 10.1021/acs.estlett.9b00612
Environ. Sci. Technol. Lett. 2019, 6, 745−751

(57) Schock, M. R.; Cantor, A. F.; Triantafyllidou, S.; Desantis, M. K.; Scheckel, K. G. Importance of Pipe Deposits to Lead and Copper Rule Compliance. *J. - Am. Water Works Assoc.* **2014**, *106*, E336−E349.

DOI: 10.1021/acs.estlett.9b00612
Environ. Sci. Technol. Lett. 2019, 6, 745−751